CrystEngComm

Accepted Manuscript

ROYAL SOCIETY OF CHEMISTRY

www.rsc.org/crystengcomm

Cite this: DOI: 10.1039/c0xx00000x

www.rsc.org/xxxxxx

PAPER

Bilayer architecture based on hexanuclear heterometal cluster units

Wei-Hui Fang and Guo-Yu Yang*

Received (in XXX, XXX) Xth XXXXXXXXX 20XX, Accepted Xth XXXXXXXXX 20XX
DOI: 10.1039/b000000x

The first bilayer architecture based on hexanuclear heterometal cluster units, $[EuCu^{II}_2Cu^{I}(\mu_3\text{-}OH)(\mu\text{-}OH)L_4(ClO_4)(H_2O)]\cdot ClO_4\cdot 3H_2O$ (**1**, L = 4-pyridin-4-yl-benzoate) was hydrothermally made and characterized. One prominent feature is the nodes are heteralmetal hexanuclear clusters ($Eu^{III}_2Cu^{II}_4$) rather than mono-metal ions, in which the heterometal clusters are in "head-to-head" arrangement. Another feature is the linkages between monolayers: instead of the generally organic linkers, the linkers here are $[Cu^{I}L_2]$ motifs. Moreover, their orientation is opposite: the organic linkers in the literatures are approximately vertical to the monolayers, while the $[Cu^{I}L_2]$ motifs are parallel to the monolayers. Charge balance is achieved by both non-coordinating and coordinating ClO_4^- anions.

Introduction

Coordination polymers (CPs) are infinite systems constructed from covalent bonds and other weak chemical bonds between metal ions and organic ligands. During the past few decades, the construction of CPs have attract extensive interest in coordination chemistry and crystal engineering, not only by their potential applications,[1] but also by their fascinating architectures and topologies.[2] As a result, numerous literatures contribute in this field, and vast CPs with discrete, and extended arrays of one dimensional (1D), 2D as well as 3D have been made. Simultaneously, interesting structure motifs appear, such as linear/zigzag chains;[3] square network, bilayer;[4] diamondoid and octahedral net.[5] Bilayers can serve as large building units, once polycatenated or pillared, 3D network will be received. In fact, bilayer could also be found in inorganic frameworks of borates and silicates.[6] The inorganic single layers were connected by sharing oxygen atoms[7] or clusters[8] to form inorganic double layers. But in inorganic-organic hybrid material, the monolayers were extended by organic ligands. Thus, multidentate ligands like oxalate,[9] isonicotinate,[10] trimesate,[11] and derivations of 4,4'-biphenyl[12] have been extensively employed.

Heterometallic clusters/CPs with different metals may induce multi-functionality, which make them more interesting than the homometallic ones.[13] So far, many heterometallic compounds and bilayer architectures based on transition-metal (TM) or lanthanide (Ln) ions have been reported.[9,13,14] However, the heterometallic bilayer are still very scarce, especially the bilayers based on heterometal clusters. Thus, it remains a synthetic challenge due to the competitive reactions between Ln and TM chelating to the same ligand, and the rational assembly of the oriented bilayers built by the cluster units. In this case, supporting ligands require an adequate number of binding sites and capacity to link both Ln and TM together. Aromatic carboxylate ligand, 4-pyridin-4-yl-benzoic acid (HL) seems good candidate: 1) It is a rigid ligand with O and N donors on opposite sides, enabling the L ligand to act as a linear bridge; 2) the carboxylate oxygen atoms (O_{COO}-) may coordinate to the oxophilic Ln ions, the pyridyl nitrogen atoms (N_{PY}) can bridge to TM ions, and thus extended heterometallic framework might be obtained; 3) besides covalent bonds between metal ions and organic ligands, weak interaction may exist: N_{PY} and the O_{COO}- atoms can participate in hydrogen bonds and the aromatic rings allow intermolecular π-π stacking interactions. By this ligand, a bipillared-bilayer TM CP based on L ligands was reported.[15] With respect to the TM bilayer, we focus Ln-containing analogues. Recently, we have afforded a series of Ln bilayers built by heptanuclear Ln cluster units with *hxl* net.[16] As an expansion of our work, we speculate that the combined introduce of Ln and TM under rational conditions may promote the formation of heterometal bilayers. Inspired by the above speculation and consideration, a novel heterometal bilayer, $[EuCu^{II}_2Cu^{I}(\mu_3\text{-}OH)(\mu\text{-}OH)L_4(ClO_4)(H_2O)]\cdot ClO_4\cdot 3H_2O$ (**1**) was made. So far, it represents the first example of bilayer based on hexanuclear heterometal clusters. Generally, bilayers can be fabricated by T-shaped,[11a,12a,17] rectangular[10,11b,12b,18] and other types building blocks.[19] In contrast to the classic T-shaped bilayers, compound **1** is a rhombic grid bilayer (Scheme 1).

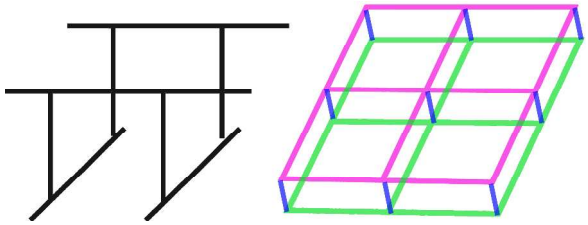

Scheme 1 Schematic diagrams present T-shaped and rhombic grid bilayers.

Experimental section

Materials and physical measurements

All chemicals were commercially purchased and used without further purification. The elemental analyses (C, H and N) were performed on a Vario EL III elemental analyzer. The FT-IR spectrum (KBr pellets) was recorded by using an ABB Bomen MB 102 spectrometer over a range 400-4000 cm^{-1}. Thermogravimetric analysis (TGA) was performed on a Mettler TGA/SDTA 851^e analyzer with a heating rate of 10 ºC/min from 30 to 1000 ºC under air atmosphere. Powder X-ray diffraction (PXRD) data were collected on a Rigaku Mini Flex II diffractometer using CuK_α radiation (λ = 1.54056 Å) under ambient conditions. Photoluminescence analyses were performed on an Edinburgh Instrument F920 fluorescence spectrometer. UV/Vis diffuse reflectance spectral measurements were carried out using a Perkin-Elmer Lambda 950 spectrometer.

Synthesis of compound 1

A mixture of $Eu(ClO_4)_3{\cdot}6H_2O$ (0.2 mmol, 0.112 g), $Cu(OH)_2$ (0.5 mmol, 0.050 g), HL(0.5 mmol, 0.099 g), and H_2O (10.0 mL 0.22 mmol) was sealed in a 30 mL Teflon-lined bomb at 200 °C for 7 days, and then cooled to room temperature. Blue plate crystals of **1** were recovered by filtration, washed with distilled water and dried at ambient temperature (Yield 36% based on $Eu(ClO_4)_3{\cdot}6H_2O$). Elemental analysis (%) Calcd. for $C_{48}H_{42}Cl_2Cu_3EuN_4O_{22}$: C 40.03, H 2.94, N 3.89. Found: C 40.88, H 3.36, N 3.87. IR (KBr pellet, cm^{-1}): 3409(s), 2356(w), 1593(vs), 1556(vs), 1404(vs), 1224(w), 1078(s), 1010(w), 835(w), 783(m), 735(w), 626(m).

X-ray crystallography study

The intensity data collected at 293 K on a SuperNova, Dual, Atlas diffractometer with graphite-monochromatized CuK_α radiation (λ = 1.54178 Å). The structure was solved with the *ShelXS* structure solution program using Direct Methods and refined with the *ShelXL* refinement package using Least Squares minimisation.[20] Non-hydrogen atoms were refined anisotropically. The positions of hydrogen atoms were generated geometrically and allowed to ride on their parent atoms. Selected bond lengths are listed in Table S1.

Results and discussion

Synthesis

To construct 3d-4f heterometal CPs, one fundamental problem should be settled, that is how to harmonize the competition between TM and Ln ions, as homometal CPs rather than heterometal complexes are usually received when chelating to the same ligand. Thus, multi-functional HL ligand with mixed N/O donors is introduced, and reasonable assembly *via* appropriate synthesis method is necessary. To date, saturation, diffusion and hydro(solvo)thermal methods are three main synthetic strategies.[2a] When close to room temperature, the slow evaporation/diffusion of solvent is often adopted to control the reaction rate and single crystals growth. At higher temperature, hydro(solvo)thermal approach, which can usually reduce reaction times, is applied. By this feasible and convenient hydrothermal synthesis, abundant heterometallic phases have been achieved in our laboratory.[21] In the process of syntheses, not only judicious choice of raw materials and bridging ligands, but also careful controls of compositional and process parameters are required.

Since the solubility of HL is small in water, hydrothermal technique is employed.[14,15,22] In our previous work, Ln oxide and copper halide were chosen as the source of Ln and TM, respectively. As a result, two types of metal cores, Ln oxo clusters and copper halide motifs, are usually incorporated in the structure. To obtain heterometal CPs constructed from only one kind of heterometal cores, which differs from our former work, copper hydroxide rather than copper halide is adopted as the TM component here. It is reported that the introduction of Cu^{II} in the framework allows flexible coordination modes and obvious Jahn-Teller distortion,[23] which provide possibilities for further aggregation of Ln and copper ions simultaneously. The Cu^{II} cations could be reduced to the Cu^{I} ions under hydrothermal conditions, resulting in the mixed-valence Cu^{I}/Cu^{II} species formed in-situ.[24] Although Cu^{II} ions are used as starting materials, analysis of the Cu-O/N bond distances, charge balancing, and bond valence sum calculations[25] all indicate that Cu1 and Cu2 ions are divalent while Cu3 ions are monovalent (Table S2). Comparison experiments have been carried out during this period of research: crystals are observed by changing basic cupric carbonate as copper source under the same reaction conditions; no crystals are found when $Eu(ClO_4)_3$ are replaced by other Ln salts. In literature, perchlorate groups as the counteranions are either free anions or coordinating (decorating/bridging) groups.[26] In this text, not only free, but also decorating ClO_4^- groups are both included in the structure. It was also noteworthy that the amount of $Eu(ClO_4)_3$ and $Cu(OH)_2$ should be limited. Too much $Cu(OH)_2$ and $Eu(ClO_4)_3$ led to only precipitation and solution, respectively.

Structure of compound 1

Single-crystal X-ray diffraction analysis[27] reveals that **1** exhibits bilayer architecture and crystallizes in the triclinic system with *P*1 space group. There are one Eu^{III} ion, two Cu^{II} ions, one Cu^{I} ion, two hydroxyls, four L ligands, two (one free and one decorating) perchlorate, one coordinated and three lattice water molecules in the asymmetric unit (Fig. 1a). The coordination polyhedron around the Eu^{III} ion can be visualized as distorted square antiprism geometry with a EuO_8 coordination mode: six O_{COO}- from six L anions, one hydroxyl group and one coordinate

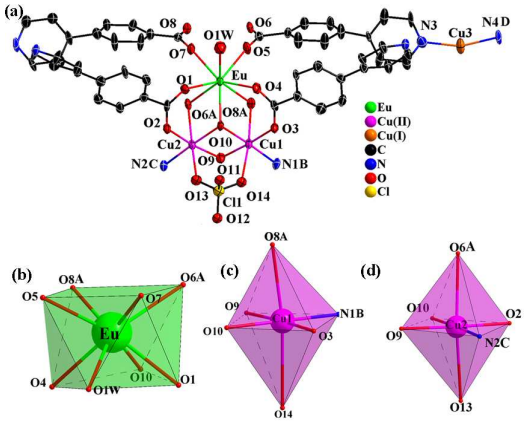

Fig. 1 (a) The asymmetric unit of compound **1**. The guest ClO_4^- and lattice water molecules are omitted for clarity. (b-d) The coordination

environments of Eu and Cu ions. Symmetry codes: A: -*x*+2, -*y*+1, -*z*; B: *x*, *y*-1, *z*; C: *x*, *y*, *z*-1; D: *x*, *y*-1, *z*+1.

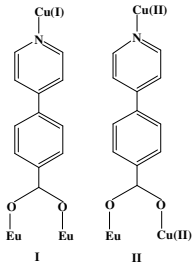

Scheme 2 Coordination modes of the L ligands.

water molecule (Fig. 1b,S1). The Eu-O distances range from 2.361(7) to 2.506(9) Å (Table 2), which are comparable to related europium complexes.[28] Owing to the Jahn-Teller distortion of Cu^{II} ions in the crystal field, the weak Cu-O interactions will be considered. The Cu^{II} (Cu1 and Cu2) ions adopt axially elongated octahedral geometry, and the axial Cu-O bonds (2.502(7)-2.842(3) Å) are much longer than the equatorial Cu-O or Cu-N bonds (Cu-O: 1.932(6)-1.976(7); Cu-N: 1.982(8)-2.010(9) Å) (Fig. 1c,d,S2). The Cu^{I} centre (Cu3) has a nonlinear coordination environment comprising of two N_{PY} with Cu-N distances of 2.036(1) and 2.030 (5) Å, and N-Cu-N angles of 160.2(7)°. Thus formed $[Cu^{I}L_2]$ motif can also be observed in our reported pillared-layer 3d-4f heterometal frameworks based on tetranuclear Ln clusters.[21d] Remarkably, it represents the first example that N_{PY} of L ligands can coordinate to Cu^{I} and Cu^{II} ions. In the structure, the L ligands exhibit μ_3-L-κ^1N,κ^1O,κ^1O' (mode I and II) coordination modes (Scheme 2). Mode II is a new coordination mode according to the Cambridge Structural Database (CSD, Version 5.34, Feb 2014 update), and represents rare example that Cu^{II} and Ln ions are simultaneously bridged by O_{COO}- atoms of L ligands (Scheme S1).[29]

Eu^{III} and Cu^{II} ions are capped by μ_3-OH that lies slightly (0.77 Å) out of the plane to produce a heterometallic triangle $[Eu^{III}Cu_2^{II}(\mu_3\text{-OH})]^{6+}$ ($Eu^{III}Cu_2^{II}$) (Fig. 2a). Notice that the Jahn-Teller effect results in the axial elongation of two adjacent octahedral Cu^{II} ions, which further stabilize the heterometal triangles. With respect to the triangle plane, the Eu···Cu1, Eu···Cu2, and Cu1···Cu2 separation is approximately of 3.578(2), 3.601(2) and 2.952(2) Å. These heterometal triangles associated with the L ligands in mode II originates monolayer on the *bc* plane with a thickness of 6.3 Å (Fig. 3a,S3). Such monolayer can be rationalized as a 4-connected *sql* net considering heterometallic triangles as nodes. When viewed down along the *a* axis, there are approximately rectangular channels with dimensions of 14.71×19.53 Å, where uncoordinated perchlorate and lattice water molecules are located. Moreover, two adjacent symmetry-related monolayers are further linked by $[Cu^{I}L_2]$ motifs to generate a 2D bilayer with a distance of 3.9 Å between the two monolayers (Fig. 3b,c). Decorated

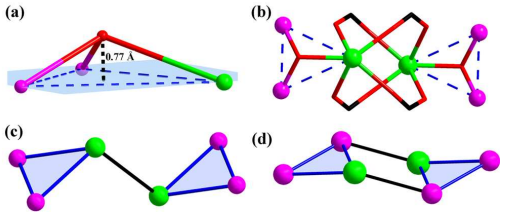

Fig. 2 (a-b) Ball stick view of the $Eu^{III}Cu_2^{II}$ and $Eu^{III}_2Cu^{II}_4$ cores; (c-d) Schematic representation of metal skeleton for **1** and ref. 31.

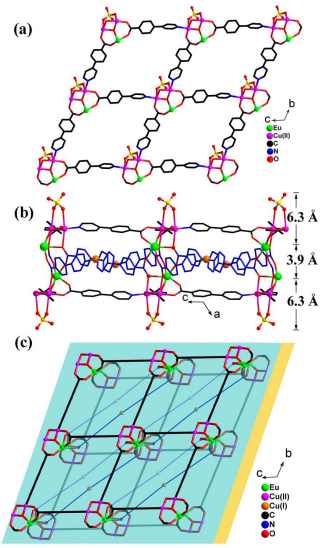

Fig. 3 (a) The cationic monolayer. (b-c) Side and top view of the bilayer architecture. The perchlorate groups are omitted for clarity. And the benzene and pyridine rings of L ligands are shown in blue and black lines, respectively.

perchlorate hang on both sides of the bilayer and pointing to the space of adjacent bilayers. Different from the reported T-shaped bilayer, this is, to the best of our knowledge, the first example of bilayer architecture based on rhombic grids assem-bled *via* hexanuclear heterometal clusters.

From another perspective, such bilayer architecture can be viewed as an extension of the hexanuclear heterometal cluster building units. It is reported that heterometallic triangles could be served as second building unit to various high-nuclearity hetero-metal clusters.[30] In this text, the Eu^{III} ions of two parallel triangles are captured by four L ligands in mode I resulting in a "head-to-head" hexanuclear hetero-metal cluster $[Eu^{III}_2Cu^{II}_4(CO_2)_4(\mu_3\text{-OH})_2]^{8+}$ ($Eu^{III}_2Cu^{II}_4$) (Fig. 2b,c). It should be mentioned that the metal skeleton in **1** is quite different from the reported Ln_2Cu_4 cases,[31] in which two triangles are linked each other to give an "edge-to-edge" arrangement (Fig. 2d). The distance (1.395 Å) of the two parallel triangles in "edge-to-edge" is much short than that (4.207 Å) in "head-to-head" arrangement. As many as twelve L ligands bonded to the heterometallic $Eu^{III}_2Cu^{II}_4$ core, four ligands are in mode I and the other eight are in mode II (Fig. S4). Each $Eu^{III}_2Cu^{II}_4$ core is connected to four nearest ones through eight L ligands in mode II with the distances of 15.5 Å (Fig. 4a). In addition, every $Eu^{III}_2Cu^{II}_4$ cluster is further linked by four $[Cu^{I}L_2]$ motifs to other two neighbours with a distance up to 25.1 Å (Fig. 4b). Hence, the framework **1** defined as a six connected uninodal *hxl* net with schläfli symbol ($3^6.4^6.5^3$) (Fig. 4c).

To avoid steric hindrance, adjacent bilayers stacked in staggered arrangement create channels, in which guest water molecules and ClO_4^- groups reside. The structures possess significant hydrogen bonds, as well as π-π interactions. The guest water molecules are engaged in hydrogen bonds with hydroxyl groups of trinuclear cores (O9-H···O2W,O10-H···O3W) and O_{COO}- from L ligands (O4W-H···O5) (Fig. S5,Table S3). In addition, the bilayers are stacked by weak π-π stacking to give 3D

supermolecular (Fig. 5). The perpendicular distance between the

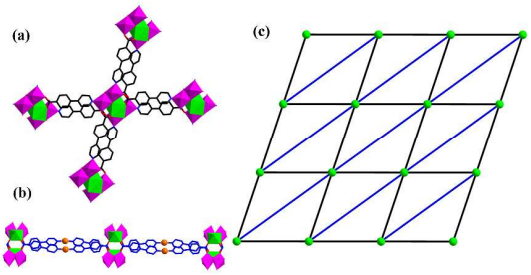

Fig. 4 (a-b) The linkage of $Eu^{III}_2Cu^{II}_4$ core. L ligands in mode II and I are shown in black and blue. The decorating perchlorate are omitted for clarity; (c) Schematic representation of the 6-connected uninodal *hxl* net.

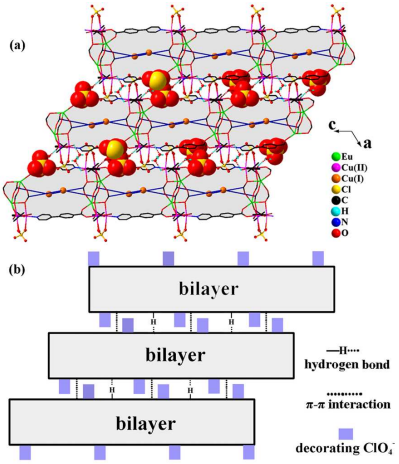

Fig. 5 (a) The packing arrangement of compound **1** along the *b* axis. The guest perchlorate are emphasized in space-filling; (b) An idealized view of the 3D sandwich supramolecular.

phenyl and pyridyl groups on a neighbouring bilayers is 3.9 Å. Thus, the weak inter-actions of π-π stacking and hydrogen bonds play critical roles in stabilizing the crystal structure.

When referred to pillared-layer frameworks, the pillars usually run vertically to the layers.[22a] Similar phenomenon can be observed in our previous work based on isonicotinic acid (HIN) and HL.[21b,d,e,28c] From the linkers point of view, bilayers are almost linked by organic li-gands.[14,15,17-19] Note that the linkers between the monolayers here are $[CuL_2]$ motifs. Moreover, the organic linkers in the literatures are approximately vertical to the monolayers, while the $[CuL_2]$ motifs are parallel to the monolayers here. Such bilayer network with a total thickness of approximately 1.6 nm remained us a type of 3D microporous layered materials,[6b,7] which was first proposed in silicate AMH-3.[6b] Porous materials are interesting for they will allow fast transport but keep desirable properties and open up the avenue to combined microporous-mesoporous materials. In this respect, new materials will be obtained in the future if these porous layers are reasonably controlled and tailored.

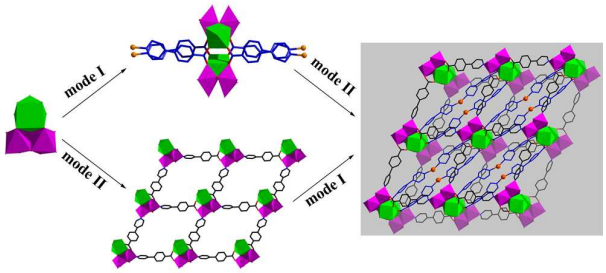

Fig. 6 The assembly pathway of the bilayer. The decorating perchlorate are omitted for clarity.

The successful synthesis of the bilayer architecture suggests that two classes of heterometallic CPs can be made by this multi-functional L ligand in our system: one contains two types of Ln and TM cores in our previous work;[21d,e] another is made up of only one kind of heterometal clusters in this paper. However, it is difficult to explain the exact route of the assembly: whether gathering into hexa-Ln cluster at the beginning or connecting into monolayers first, but it is clear that the axially elongated octahedral geometry of Cu^{II} ions resulting from Jahn-Teller distortion plays an important role in the structural construction (Fig. 6).

Comparison of structures

Compound **1** shares structural commonalities and differences with our previous reported bilayer based on heptanuclear Ln cores[16] (denoted **1'**, Fig. 7,S6). Firstly, the subunits in these two layers are both trinuclear units of defected cubane: heterometallic $Eu^{III}Cu^{II}_2$ in **1** and homometallic Ln^{III}_3 in **1'**. Secondly, the subunits are inter-linked by L ligands to 4- and 6-connected single layers in **1** and **1'**, respectively. Thirdly, the monolayers here are integrated by parallel $[Cu^{I}L_2]$ pillars, whereas in **1'** they are linked by Ln ions, and are further stabilized by terminal L ligands. Finally, these bilayers both display 6-connected *hxl* topology. Though there are two types of coordination modes in these two compounds, their functions are different: the combined work of L ligands in mode I and II leads to the formation of **1**, while compound **1'** are exclusively connected by one type of L ligands, the other type just assist and stabilize the bilayer.

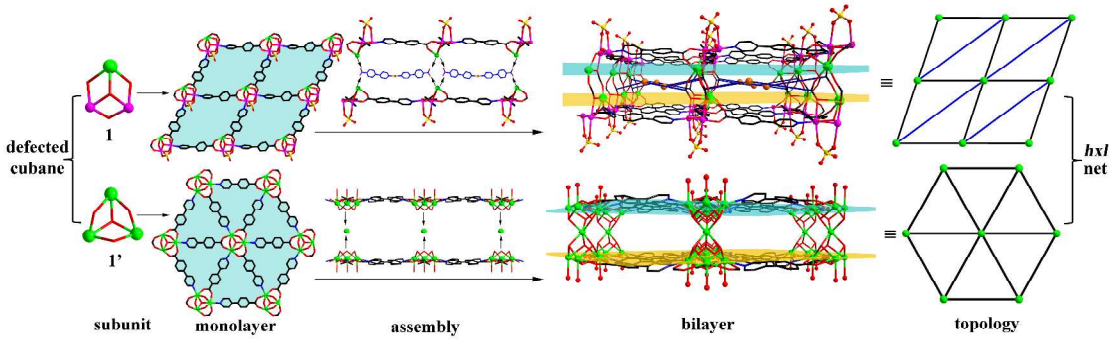

Fig. 7 The scheme diagram of the comparisons between **1** and **1'** (ref. 16). The terminal L ligands in **1'** are omitted for clarity.

PXRD, IR spectroscopy and TGA

Simulated and experimental PXRD patterns (Fig. S7) of **1** well match each other, indicating the phase purity of the bulk sample. The characteristic features of carboxylates dominate the IR spectrum (Fig. S8), in which the strong and characteristic Cl-O stretching frequencies around 1078 cm^{-1} and 626 cm^{-1} are also observed. TG curve (Fig. S9) undergoes two steps of weight loss during 30-500°C. The slight weight increase above 500 °C might be attributed to the oxidation of Cu^{I} to Cu^{II} under air atmosphere. Assuming the residue composition corresponds to Eu_2O_3 and CuO, the observed weight (28.9%) is in good agreement with the calculated value (28.8%).

Luminescence properties

Solid-state photoluminescent emission spectrum of **1** was measured at room temperature near visible region (350-800 nm) (Fig. S10). The characteristic $^5D_0 \rightarrow {}^7F_J$ (J = 0-4) transition of Eu^{3+} ions at about 579, 590, 613 648 and 698 nm was not observed because water quenches the lanthanide luminescence. The emission peak at 425 nm can be assigned to the ligand-centered fluorescence. The red shift (HL 416) may be attributed to the ligand-to-metal charge transfer (LMCT).

UV/Vis absorption spectra

The UV-vis-IR absorption spectrum is calculated from the data of diffuse reflectance using the Kubelka-Munk function.[32] Besides the local band of the L ligands at 279 nm, a broad band corresponding to the d-d transition of the Cu^{II} ions is observed at 700 nm. In the F(R) and E(eV) plot, the band gap is 3.7 eV (Fig. 8).

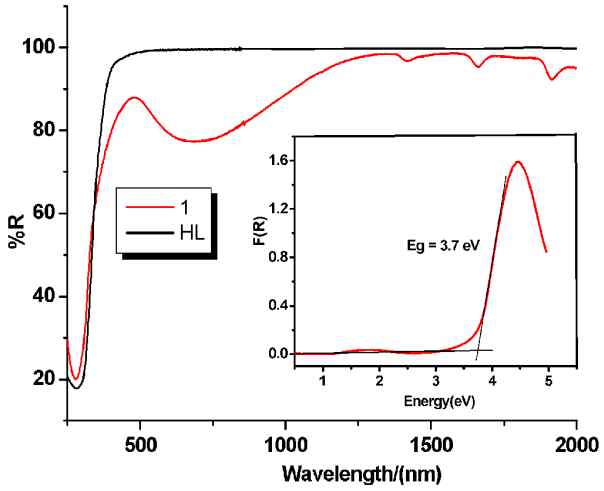

Fig. 8 UV-vis-IR optical diffuse reflectance spectra for **1**.

Conclusion

In conclusion, the synthesis, structure and characterization of a heterometallic CP with an unusual bilayer structure has been made under hydrothermal conditions. The distinctive features of the structure involve both the nodes and the linkers: the metal nodes in this paper are heterometal clusters rather than metal ions; the orientation of the novel $[Cu^{I}L_2]$ motif linkers is parallel instead of vertical to the monolayers. Remarkably, it is the first bilayer architecture based on hexanuclear heterometal cluster units. This work enriches the class of heterometal CPs in the Ln-Cu-L system, further suggests that the L ligand provides the potential to generate bilayer architectures.

Acknowledgements

This work was supported by the NSFC (Nos. 91122028, 21221001, and 50872133), the 973 Program (Nos. 2014CB932-101 and 2011CB932504), the NSFC for Distinguished Young Scholars (No. 20725101).

Notes and references

State Key Laboratory of Structural Chemistry, Fujian Institute of Research on the Structure of Matter, Chinese Academy of Sciences, Fuzhou, Fujian 350002, China. Fax:+86-591-83710051;E-mail: ygy@fjirsm.ac.cn.

† Electronic Supplementary Information (ESI) available: XRD, IR, TGA, emission spectra and additional Fig.s and tables. CCDC reference number 955407 (**1**). For ESI and crystallographic data in CIF or other electronic format see DOI: 10.1039/ b000000x/

1 (*a*) C. Wang, T. Zhang and W. Lin, *Chem. Rev.,* 2012, **112**, 1084; (*b*) D. Bradshaw, J. B. Claridge, E. J. Cussen, T. J. Prior and M. J. Rosseinsky, *Acc. Chem. Res.,* 2005, **38**, 273; (*c*) M. D. Allendorf, C. A. Bauer, R. K. Bhakta and R. J. T. Houk, *Chem. Soc. Rev.,* 2009, **38**, 1330; (*d*) M. Kurmoo, *Chem. Soc. Rev.,* 2009, **38**, 1353.

2 (*a*) A. Y. Robin and K. M. Fromm, *Coord. Chem. Rev.,* 2006, **250**, 2127; (*b*) D. L. R. J. Hill, N. R. Champness, P. Hubberstey and M. Schröder., *Acc. Chem. Res.,* 2005, **38**, 337.

3 (*a*) G. Calvez, C. Daiguebonne and O. Guillou, *Inorg. Chem.,* 2011, **50**, 2851; (*b*) Y. Q. Sun, J. Zhang, J. L. Chen and G. Y. Yang, *Eur. J. Inorg. Chem.,* 2004, 3837.

4 (*a*) E. Q. Gao, Y. X. Xu and C. H. Yan, *CrystEngCommun,* 2004, **6**, 298; (*b*) M. Kondo, T. Yoshitomi, K. Seki, H. Matsuzaka and S. Kitagawa, *Angew. Chem., Int. Ed. Engl.,* 1997, **36**, 1725.

5 (*a*) J. Zhang and X. H. Bu, *Angew. Chem., Int. Ed.,* 2007, **46**, 6115; (*b*) S. Noro, S. Kitagawa, M. Kondo and K. Seki, *Angew. Chem., Int. Ed.,* 2000, **39**, 2081.

6 (*a*) C. T. Chen, Y. B. Wang, B. C. Wu, K. C. Wu, W. L. Zeng and L. H. Yu, *Nature,* 1995, **373**, 322; (*b*) H. K. Jeong, S. Nair, T. Vogt, L. C. Dickinson and M. Tsapatsis, *Nat. Mater.,* 2003, **2**, 53.

7 D. B. Xiong, J. T. Zhao, H. H. Chen and X. X. Yang, *Chem.-Eur. J.,* 2007, **13**, 9862.

8 L. Cheng, Q. Wei, H.-Q. Wu, L.J. Zhou and G.-Y. Yang, *Chem.-Eur. J.,* 2013, **19**, 17662.

9 P. C. Soares-Santos, L. Cunha-Silva, F. A. Paz, R. A. Ferreira, J. Rocha, L. D. Carlos and H. I. Nogueira, *Inorg. Chem.,* 2010, **49**, 3428.

10 Z. Y. Fu, X. T. Wu, J. C. Dai, L. M. Wu, C. P. Cui and S. M. Hu, *Chem. Commun.,* 2001, 1856.

11 (*a*) J. C. Dai, X. T. Wu, Z. Y. Fu, C. P. Cui, S. M. Hu, W. X. Du, L. M. Wu, H. H. Zhang and R. O. Sun, *Inorg. Chem.,* 2002, **41**, 1391; (*b*) J. C. Dai, S. M. Hu, X. T. Wu, Z. Y. Fu, W. X. Du, H. H. Zhang and R. Q. Sun, *New J. Chem.,* 2003, **27**, 914.

12 (*a*) Z. Y. Fu, X. T. Wu, J. C. Dai, S. M. Hu and W. X. Du, *New J. Chem.,* 2002, **26**, 978; (*b*) R. J. Hill, D. L. Long, M. S. Turvey, A. J. Blake, N. R. Champness, P. Hubberstey, C. Wilson and M. Schroder, *Chem. Commun.,* 2004, 1792.

13 (*a*) X. J. Kong, Y. P. Ren, W. X. Chen, L. S. Long, Z. P. Zheng, R. B. Huang and L. S. Zheng, *Angew. Chem. Int. Ed.*, 2008, **47**, 2398; (*b*) D. Sun, D. F. Wang, X. G. Han, N. Zhang, R. B. Huang and L. S. Zheng, *Chem. Commun.,* 2011, **47**, 746; (*c*) B. Zhao, X. Y. Chen, P. Cheng, D. Z. Liao, S. P. Yan and Z. H. Jiang, *J. Am. Chem. Soc.*,

2004, **126**, 15394; *(d)* B. Zhao, X. Y. Chen, Z. Chen, W. Shi, P. Cheng, S. P. Yan and D. Z. Liao, *Chem. Commun.*, 2009, 3113.

14 (*a*) Y. L. Zhou, M. C. Wu, M. H. Zeng and H. Liang, *Inorg. Chem.,* 2009, **48**, 10146; (*b*) M. H. Zeng, S. Hu, Q. Chen, G. Xie, Q. Shuai, S. L. Gao and L. Y. Tang, *Inorg. Chem.,* 2009, **48**, 7070.

15 Z. Yin, Q. X. Wang and M. H. Zeng, *J. Am. Chem. Soc.,* 2012, **134**, 4857.

16 W. H. Fang, L. Cheng, L. Huang and G. Y. Yang, *Inorg. Chem.,* 2013, **52**, 6.

17 M. J. Zaworotko, *Chem. Commun.,* 2001, 1.

18 J. J. Wang, L. Gou, H. M. Hu, Z. X. Han, D. S. Li, G. L. Xue, M. L. Yang and Q. Z. Shi, *Cryst. Growth Des.,* 2007, **7**, 1514.

19 (*a*) A. Dimos, A. Michaelides and S. Skoulika, *Chem. Mater.,* 2000, **12**, 3256; (*b*) X. Y. Cao, J. Zhang, Z. J. Li, J. K. Cheng and Y. G. Yao, *CrystEngComm,* 2007, **9**, 806.

20 (*a*) G. M. Sheldrick, *SHELXS97*, *Program for Crystal Structure Solution;* University of Göttingen: Göttingen, Germany, **1997**; (*b*) G. M. Sheldrick, *SHELXL97*, *Program for Crystal Structure Refinement;* University of Göttingen: Göttingen, Germany, **1997**.

21 (*a*) M. B. Zhang, J. Zhang, S. T. Zheng and G. Y. Yang, *Angew. Chem., Int. Ed.,* 2005, **44**, 1385; (*b*) J. W. Cheng, J. Zhang, S. T. Zheng, M. B. Zhang and G. Y. Yang, *Angew. Chem., Int. Ed.,* 2006, **45**, 73; (*c*) J. W. Cheng, S. T. Zheng, W. Liu and G. Y. Yang, *CrystEngComm,* 2008, **10**, 1047; (*d*) W. H. Fang and G. Y. Yang, *CrystEngComm,* 2013, **15**, 9504; (*e*) W. H. Fang, J. W. Cheng and G. Y. Yang, *Chem.-Eur. J.,* 2014, **20**, 2704.

22 (*a*) M. H. Zeng, Y. L. Zhou, M. C. Wu, H. L. Sun and M. Du, *Inorg. Chem.,* 2010, **49**, 6436; (*b*) Y. P. He, Y. X. Tan and J. Zhang, *CrystEngComm,* 2012, **14**, 6359.

23 (*a*) B. Li, J. W. Zhao, S. T. Zheng and G. Y. Yang, *Inorg. Chem.,* 2009, **48**, 8294; (*b*) J. W. Zhao, C. M. Wang, J. Zhang, S. T. Zheng and G. Y. Yang, *Chem.-Eur. J.,* 2008, **14**, 9223.

24 L. Hou, D. Li, W. J. Shi, Y. G. Yin and S. W. Ng, *Inorg. Chem.,* 2005, **44**, 7825.

25 I. D. Brown and D. Altermatt, *Acta Crystallogr., Sect. B: Struct. Sci.,* 1985, **41**, 244.

26 (*a*) D. Das, B. Sarkar, T. K. Mondal, S. M. Mobin, J. Fiedler, W. Kaim and G. K. Lahiri, *Inorg. Chem.,* 2011, **50**, 7090; (*b*) P. P. Chakrabarty, D. Biswas, S. Garcia-Granda, A. D. Jana and S. Saha, *Polyhedron,* 2012, **35**, 108; (*c*) Q. T. He, X. P. Li, Y. Liu, Z. Q. Yu, W. Wang and C. Y. Su, *Angew. Chem., Int. Ed.,* 2009, **48**, 6156.

27 Crystal data for **1**: $C_{48}H_{42}Cl_2Cu_3EuN_4O_{22}$, M_r = 1440.34, triclinic, *P*1, *a* = 15.026(9) Å, *b* = 15.473(9) Å, *c* = 15.512(9) Å, α = 108.495(5) º, β = 117.49 º, γ = 96.862(6) º, *V* = 2879(3) Å^3, *Z* = 2, ρ = 1.667 g cm^{-3}, μ = 2.339 mm^{-1}, *F* (000) = 1436, GOF = 1.050. Of total 18482 reflections collected, 9913 are unique (R_{int} = 0.0651). R_1/wR_2 = 0.0882/0.2165 for 6934 reflections and 740 parameters (I>2σ(I)).

28 (*a*) J. W. Cheng, S. T. Zheng, E. Ma and G. Y. Yang, *Inorg. Chem.,* 2007, **46**, 10534; (*b*) J. W. Cheng, S. T. Zheng and G. Y. Yang, *Dalton Trans.,* 2007, 4059; (*c*) J. W. Cheng, J. Zhang, S. T. Zheng and G. Y. Yang, *Chem.-Eur. J.,* 2008, **14**, 88.

29 M. B. Zhang, H. M. Chen, R. X. Hu and Z. L. Chen, *CrystEngComm,* 2011, **13**, 7019.

30 (*a*) A. J. Blake, P. E. Y. Milne, P. Thornton and R. E. P. Winpenny, *Angew. Chem., Int. Ed. Engl.,* 1991, **30**, 1139; (*b*) T. N. Hooper, J. Schnack, S. Piligkos, M. Evangelisti and E. K. Brechin, *Angew. Chem., Int. Ed.,* 2012, **51**, 4633.

31 S. L. Cai, S. R. Zheng, Z. Z. Wen, J. Fan and W. G. Zhang, *Cryst. Growth Des.,* 2012, **12**, 5737.

32 (*a*) P. Kubelka and F. Z. Munk, *Tech. Phys.,* 1931, **12**, 593; (*b*) W. W. Wendlandt and H. G. Hecht, *Reflectance Spectroscopy*; Wiley-Interscience, New York, **1966**.

Entry for the Table of Contents:

An unprecedented bilayer architecture based on "head-to-head" hexanuclear heterometal clusters and linked by parallel [$Cu^{I}L_2$] motifs has been hydrothermally made.